A Measurement of the Yield of Carbon Monoxide from the Reaction of Methyl Radicals and Oxygen Atoms

Jack M. Preses* and Christopher Fockenberg†

Chemistry Department 555A, Brookhaven National Laboratory, P.O. Box 5000 Upton, New York 11973-5000

George W. Flynn‡

Department of Chemistry, Columbia University, New York, New York 10027

Received: February 2, 2000; In Final Form: May 22, 2000

We have determined the branching fraction for the production of CO from the reaction of methyl radicals and $O(^3P)$ atoms at room temperature to be 0.18 ± 0.04 at $T = 296$ K. The measurement was made by determining the concentration of CO using tunable infrared diode laser absorption. Methyl radicals and O atoms were prepared by 193-nm excimer laser photolysis of acetone and SO_2. CO produced directly from acetone photolysis was distinguished from that generated by the radical−radical reaction by using acetone labeled with ^{13}C only on the methyl groups. The result is in excellent agreement with another determination of the CO branching fraction made using time-of-flight mass spectrometry.

Introduction

In a recent publication from our laboratory,[1] the room-temperature rate constant and product distribution from the reaction of methyl radicals and ^3P oxygen atoms, a reaction of pivotal importance in the combustion of hydrocarbon fuels, was examined. Possible channels include:

$$CH_3 + O(^3P) \rightarrow CH_2O + H \qquad \Delta H = -294.1 \text{ kJ/mol} \quad (1a)$$

$$\rightarrow HCO + H_2 \qquad \Delta H = -354.2 \text{ kJ/mol} \quad (1b)$$

$$\rightarrow CO + H + H_2 \qquad \Delta H = -228.7 \text{ kJ/mol} \quad (1c)$$

$$\rightarrow CH + H_2O \qquad \Delta H = -43.9 \text{ kJ/mol} \quad (1d)$$

$$\rightarrow OH + CH_2 \qquad \Delta H = +29.2 \text{ kJ/mol} \quad (1e)$$

Reports of the relative importance of reactions (1a−e) vary; in particular, the yield of CO from the reactions (1) is the subject of some controversy. We recently attempted to determine the relative yields of these reactions at room temperature using our time-of-flight mass-spectrometry (TOFMS)-based combustion kinetics apparatus.[2] Although a number of different sources contributed to the signal at mass 28, our measurements indicated a CO branching fraction of 0.17 ± 0.11. In contrast to this result, Slagle et al.[3] reported that channel (1a) is the only important one between 294 and 900 K, while Seakins and Leone[4] provided the first evidence that the sole important product of reactions (1) is not formaldehyde by measuring an overall CO yield of 0.4 ± 0.2 at room temperature. The latest version (3.0) of GRI-Mech[5] models natural gas combustion using a CO yield of 0.4, and therefore depends to some extent on this value. To estimate the magnitude of its influence, we calculated concentration profiles in a simple combustion system (adiabatic combustion of a 9% CH_4-in-air mixture at 2000 K) using GRI-Mech 3.0 and the Chemkin-II[6] kinetics package. The simulation indicates that, e.g., varying the CO yield from 0 to 0.4 results in ∼10% changes in maximum HCO and HO_2 concentrations and a few tens of degrees in final temperature.

To obtain an independent, more definitive determination of the CO branching fraction, we have determined here the CO yield using a direct, unambiguous spectroscopic method: tunable diode laser spectroscopy. The concept of the experiment is simple. A static cell is filled with premixed stable precursors to CH_3 radicals and O atoms in low concentrations, along with a bath gas. The cell is irradiated with 193-nm excimer laser radiation using a 2 Hz repetition rate to photolyze the precursors. CH_3 radicals and O atoms then react forming, among other products, CO. A diode laser tuned to a CO absorption line probes the reaction mixture after complete equilibration via bath gas collisions, which is important in order to determine accurate CO concentrations by measuring the magnitude of absorption. Comparison of the CO concentration with that of other reaction products (e.g., formaldehyde) or the initial reactant (methyl radical) concentration would then produce the CO branching fraction. In practice, however, a number of complications must be overcome to produce a valid determination of the CO yield. The O atom precursor is SO_2, and the geminate photochemical product is the SO radical, which introduces no further complications. However, the CH_3 precursor is acetone, which itself generates both CO and CH_3 by direct 193-nm photolysis, so that we must differentiate between direct photochemical CO and CO produced from the radical−radical reaction. This is accomplished by using acetone isotopically labeled with ^{13}C only on the methyl groups, a compound commercially available. Using this compound as a source of CH_3, photolytic ^{12}CO is produced directly from the acetone carbonyl and ^{13}CO must come from reactions of $^{13}CH_3$. However, ^{13}CO can also be generated from 193-nm photolysis of CH_2O produced by reaction 1a. We show below that the yield of ^{13}CO from the 193-nm photolysis of CH_2O is small and that other dark

* Corresponding author. E-mail addresses: preses@bnl.gov.
† fknberg@bnl.gov.
‡ flynn@chem.columbia.edu.

10.1021/jp000404d CCC: $19.00
Published on Web 06/28/2000

reactions that produce ^{13}CO do not contribute substantially under the conditions of our experiment. Thus, the sources of the two CO isotopologues produced from direct acetone photolysis and the CH_3 + O radical−radical reaction can be separated, and comparison of ^{12}CO and ^{13}CO concentrations is a valid measure of CO yield from the reaction of CH_3 and O atoms.

Experimental Section

The experimental apparatus is basically the same as that used in numerous previous experiments[7] and will not be described in detail here. Briefly, a lead−salt liquid-N_2 cooled diode laser was directed through a 129.5-cm-long Pyrex cell fitted with CaF_2 windows. The diode laser beam was about 0.5 cm in diameter. Unwanted diode laser modes were separated by passing the infrared beam through a monochromator. The beam was then focused onto an InSb detector. 193-nm photolysis radiation from a Questek model 2620 ArF excimer laser was counterpropagated through the cell and completely blocked from entering the diode laser by an OCLI infrared band-pass filter on a Ge substrate. The excimer laser beam was shaped to a 2-cm^2 circle using an iris before entering the cell resulting in a maximum UV laser fluence of 10 mJ/cm^2 at an overall pulse energy of 20 mJ. Absorption spectra were recorded by current-scanning the diode laser over a short ($\approx$ 0.3 cm^{-1}) spectral range where ^{12}CO and ^{13}CO absorption lines are adjacent to one another. There are two spectral regions where ^{12}CO and ^{13}CO absorption lines are next to one another and the wavelengths are accessible to the particular diode in use. Near 2073 cm^{-1} P(17) $v = 0 \rightarrow v = 1$ ^{12}C^{16}O and P(6) $v = 0 \rightarrow v = 1$ ^{13}C^{16}O are 0.26 cm^{-1} apart. Near 2077 cm^{-1} P(5) $v = 0 \rightarrow v = 1$ ^{13}C^{16}O and P(16) $v = 0 \rightarrow v = 1$ ^{12}C^{16}O are 0.29 cm^{-1} apart.[8] All of the experiments reported here were performed using the lines near 2077 cm^{-1}.

The cell is irradiated with a small number of UV pulses (typically two), three minutes are allowed for complete equilibration, and a number (typically 1000) of diode sweeps across the two IR absorption lines are averaged in a digital oscilloscope, and the result is stored on a PC. The procedure is repeated for a total of ~50 UV pulses before the cell is refilled and the whole experiment repeated.

To determine concentrations from measured absorption intensities, great care must be taken to avoid spectral distortion. For the 129.5 cm path length used in these experiments, we found empirically that in order to be free from distortion, the pressure of CO in the sample cell could not exceed ~10−15 mTorr (3.3−4.9 × 10^{14} molecules/cm^3) at 295 K in 5 Torr Ar. Premixed CO/Ar mixtures with this pressure of CO in 5 Torr Ar produced an excellent Gaussian line shape absorption for both CO transitions studied. Higher CO pressures showed evidence of flattening near the peak, i.e., all of the IR radiation has been absorbed, and, with higher CO pressures the area under the absorption line, will no longer be proportional to the CO concentration. Reaction and calibration gas mixtures were prepared at least 1 day ahead of time at a total pressure of ~1000 Torr, and the mixtures were made so that the total CO pressure in the sample cell during an experiment could not exceed 10−15 mTorr. Magnetically activated mixing vanes were inserted into the sample supply bulbs to shorten the mixing time. Acetone labeled with ^{13}C (99.5 atom %) on the methyls was obtained from Cambridge Isotope Laboratories. Air was removed from the acetone by subjecting it to three freeze−pump−thaw cycles before use. SO_2 (99.98 mass %) came from Matheson, and Ar (99.997%) from Praxair. SO_2 and Ar were used directly from the tanks.

Experiments were performed as follows. Two gas mixtures were prepared; the first mixture was 2.50 Torr natural isotopic abundance CO in 1000 Torr Ar. The second mixture was, typically, 0.80−2.50 Torr labeled acetone, 5.00−10.00 Torr SO_2, and Ar to make a total pressure of 1000 Torr. All of the experiments reported here were performed using about 5 Torr of mixtures made with acetone and SO_2 pressures at the low end of the cited ranges, making the initial acetone pressure 4 mT (1.3 × 10^{14} molecules/cm^3) and the SO_2 pressure 40 mT (1.3 × 10^{15} molecules/cm^3). The first mixture was used to determine the empirical relative sensitivity of the apparatus to the ^{12}C^{16}O and ^{13}C^{16}O lines to be used to measure CO product concentrations. The observed intensities of the two absorptions were recorded simultaneously by sweeping the diode laser across both lines and recording the absorption spectrum. Since the total pressure of CO in the calibration mixture is known, as well as the natural abundance of ^{13}C (^{12}C/^{13}C = 89.66, 1.103% ^{13}C),[9] the total line area yields an absolute calibration of experimental sensitivity to CO concentration. Irradiation of a reaction mixture (acetone, SO_2, Ar) and comparison of experimental ^{12}C^{16}O and ^{13}C^{16}O line areas with line areas from calibration measurements can then be turned into true CO concentrations. The repetition rate of the excimer laser was 2 Hz, and three minutes were allowed after irradiation to permit complete equilibration of the internal degrees of freedom and the temperature of the cell contents. For experiments where very low CO product concentrations were to be measured, a small 35 kHz sinusoidal modulation was imposed on the diode laser current (hence frequency) and signals were detected using an SRS SR830 lock-in amplifier. In this manner, reliable CO line intensities could be measured for product produced by as few as five excimer laser pulses, and every two laser pulses thereafter.

Additional experiments to determine the profile in time of ^{13}C^{16}O concentration following the excimer laser pulse were also performed (see below). For these experiments a few percent of the diode laser beam were separated from the beam used for absorption measurements using a CaF_2 beam splitter and directed through a scanning Etalon operating at a fixed spacing. A small 10 kHz sinusoidal frequency modulation was imposed on the diode laser and a second lock-in amplifier (SRS 510) was used in a feedback loop to frequency-lock the diode laser on an Etalon fringe at the center frequency of ^{13}C^{16}O. (The frequency was identified by filling the cell with 10 mT CO 50% enriched in ^{13}C^{16}O in 5 T Ar.) ^{13}C^{16}O absorption was detected with 3−30 ms time resolution depending on the setting of the time constant of the SR830 lock-in amplifier used in the signal channel. With this instrumental arrangement ^{13}C^{16}O absorption from *single* excimer laser pulses could be detected when the sample cell was filled with a reaction mixture as above.

Discussion

Analysis of the experimental data is straightforward. We measure the areas under the ^{12}CO and ^{13}CO absorption lines in a mixture of natural abundance CO and Ar at a known CO concentration. We ignore ^{18}O isotopologues. The areas under the lines are proportional to the CO concentrations and the absorption cross sections:

$$A_{12}^{\text{nat}} = C\sigma_{12}\,[^{12}\text{C}^{16}\text{O}] \tag{2a}$$

$$A_{13}^{\text{nat}} = C\sigma_{13}\,[^{13}\text{C}^{16}\text{O}] \tag{2b}$$

where A_i^{nat} represents the area under the absorption line, C is a proportionality constant, and σ_i is the absorption cross section for the line. For this mixture the actual concentration ratio [^{12}CO]/[^{13}CO] is 89.66[9] (1.103% ^{13}C abundance) so that we

can evaluate the combined constants $C \times \sigma_i$ in eqs 2. Additional calibration experiments performed with 50% enriched ^{13}CO yielded essentially the same results. We then use the evaluated constants and the measured areas under the CO lines in the reaction mixtures to determine the ^{12}CO and ^{13}CO concentrations in the reaction mixture after UV irradiation. Note that determination of the ratio of the concentrations of the CO isotopologues in the reaction mixture (hence the CO reaction yield) depends only on the *ratio* of the measured absorption line areas so that measurements of absolute quantities are not required. The absolute calibration of CO isotopologue pressures is available from this procedure, and can be used as an internal check of the data, but the determination of the CO reaction yield according to this method does not depend on absolute concentrations.

For the measurement to be valid, we must pay attention to the solution of a number of potential problems. First, radical concentrations must be adjusted so that radical−radical reactions competing with $CH_3 + O$, such as $CH_3 + CH_3$ do not distort the results. In 5 Torr Ar the rate of the methyl radical recombination reaction is 5×10^{-11} cm^3 s^{-1} at 298 K.[10] Methyl radical recombination is avoided by arranging for the concentration of CH_3 to be much smaller than that of O atoms by preparing the reaction mixture with a large (∼10-fold) excess of SO_2, the O atom precursor, compared to the initial acetone pressure. Larger SO_2 concentrations than used here to increase the [SO_2] to [acetone] ratio were not feasible because all the UV radiation would be absorbed near the front of the cell, distorting the spatial distribution (hence concentrations) of products. The cross section for absorption of 193-nm laser radiation by ^{12}C-acetone-h_6 has been measured[7] to be $3.11 \pm 0.10 \times 10^{-18}$ cm^2. While ^{13}C substitution may change this value slightly, the absorption cross section for labeled acetone will certainly be of the same order of magnitude. Because of the efficient decomposition of acetone by 193-nm radiation, measurement of the UV absorption must be performed using a cell of flowing acetone, a measurement that is too expensive to be made with the labeled compound. The 193-nm absorption cross section[11,12] of SO_2 is $\sim 6 \times 10^{-18}$ cm^2, roughly twice that for acetone. The pressures of acetone and SO_2 used in the experiments cited above are a compromise determined by the restrictions imposed on the low end by our sensitivity to detect absorptions and on the high end by the desire to achieve radical concentrations as uniform as possible along the cell axis. With the pressures of acetone and SO_2 used here, radical densities at the rear of the cell are about two-thirds those at the front of the cell. While this is of little consequence for experiments that do not measure time dependence, we do have to take axial concentration variations in cell into account when modeling time-dependence experiments.

One concern in static experiments is the possibility that the products might react further with radicals present in the reactor. Another complication involves reaction 1a. Formaldehyde produced by this reaction has been reported to absorb 193-nm radiation and to produce CO, in this case ^{13}CO that will be added to the yield of CO from the radical−radical reaction of interest.[13] We correct for any ^{13}CO yield from secondary chemistry by extrapolating the result to zero excimer laser pulses. In any event, the 193-nm absorption coefficient of formaldehyde is very small, so the ^{13}CO concentration formed from formaldehyde photolysis under these conditions is negligible. Direct attempts to quantify the 193-nm absorption coefficient of formaldehyde were not successful because it is so small. Based on a conservative estimate of our ability to detect absorption as low as ∼ 1%, an upper bound for the cross section for absorption of 193-nm radiation by formaldehyde was found to be $\sim 10^{-20}$ cm^2, a very small value, indicating a low photochemical yield of CO from this source. In addition, we also performed an experiment designed to provide some quantification of the CO yield from the 193-nm photolysis of formaldehyde. Five Torr of a premixed CH_2O/Ar mixture containing 12.4 mTorr CH_2O was irradiated with 193-nm radiation at 2 Hz for thirty minutes using the same excimer laser fluence as in the acetone experiment (∼10 mJ/cm^2, ∼20 mJ at the front window of the cell in ∼2 cm^2 area). The $^{12}C^{16}O$ concentration produced was calibrated vs. CO absorption from a known CO/Ar mixture; the CO pressure after 3600 laser pulses was 3 mTorr. A blank experiment with no CH_2O produced no discernible CO. This result indicates that the quantity of photochemical CO from CH_2O generated by the limited number of excimer laser pulses during the acetone experiment can be safely neglected. Moreover, the yield of CO from the absorption of 193-nm radiation by formaldehyde has been shown to be sensitive to laser fluence,[13] implying that multiphoton effects are important. We have been careful to maintain a low (10 mJ/cm^2) UV laser fluence, minimizing CO production from multiphoton absorption.

Although the rate constant is comparatively low, formaldehyde could react with oxygen atoms ($k = 1.7 \times 10^{-13}$ cm^3 s^{-1} at 298 K),[14] leading to highly reactive OH radicals as well as HCO, which would ultimately provide an additional source of ^{13}CO via reaction 3e between excimer laser pulses:

$$^{13}CH_3 + O \rightarrow H_2\,^{13}CO + H \quad (3a)$$

$$^{13}CH_3 + O \rightarrow {}^{13}CO + H_2 + H \quad (3b)$$

$$O + H_2\,{}^{13}CO \rightarrow OH + H^{13}CO \quad (3c)$$

$$OH + H_2\,{}^{13}CO \rightarrow H_2O + H^{13}CO \quad (3d)$$

$$H^{13}CO + O \rightarrow OH + {}^{13}CO \quad (3e)$$

$$H^{13}CO + O \rightarrow H + {}^{13}CO_2 \quad (3f)$$

$$OH + {}^{13}CH_3\,{}^{12}CO^{13}CH_3 \rightarrow \text{Products} \quad (3g)$$

$$O + SO \rightarrow \text{Products} \quad (3h)$$

We have modeled this set of reactions as follows. Using the UV absorption coefficients of acetone and SO_2 given above, we calculated the energy deposited in 130 1-cm-deep cylinders of 2 cm^2 area along the cell axis in our reaction mixture. This calculation neglects any effects of beam divergence. Assuming one-photon absorptions and complete, single-channel photolyses, this leads to initial axial density distributions of O atoms and $^{13}CH_3$ radicals. Rate constants used for reactions 3a (1.4×10^{-10} cm^3/molecule-s) and 3b (2.9×10^{-11} cm^3/molecule-s) were obtained from ref 1; for reactions 3c and 3d (2.0×10^{-13}, 1.0×10^{-11} cm^3/molecule-s) from ref 14; for reaction 3g (5.0×10^{-13} cm^3/molecule-s) from ref 15; and for reaction 3h (1.0×10^{-13} cm^3/molecule-s) from ref 16. The rate constant for reaction 3f (5.0×10^{-11} cm^3/molecule-s) was taken from ref 14, but the rate constant for reaction 3e was adjusted to 1.0×10^{-11} cm^3/molecule-s following the suggestion of Bradley and Schatz who have studied the potential energy surfaces controlling reactions of the products of reaction 3f, $H + CO_2$,[17] and $CH + O_2$.[18] The latter species can react via a direct mechanism yielding

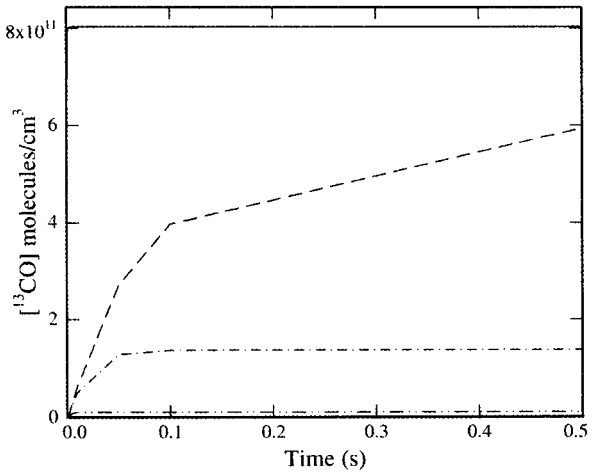

Figure 1. Modeling of the production of ^{13}CO from reactions 3. Solid line: [^{13}CO] from reaction 3b. Dashed line: [^{13}CO] produced from reactions 3d−f with the conditions cited in the text. Dot−dashed line: [^{13}CO] produced from reactions 3d−f with an additional O atom removal reaction on the cell wall with a rate constant of 50 s^{-1}. Dot−dot−dashed line: [^{13}CO] produced from reactions 3d−f with an O atom wall removal rate of 500 s^{-1}. Other rate constants are cited in the text.

HCO + O or can react via CH insertion, yielding H + CO_2 and OH + CO. By analogy, HCO + O can react directly, producing OH + CO, or it can form a HCO_2/HOCO complex, generating H + CO_2. Schatz[18] has suggested that abstraction involves a small barrier, so that at low temperatures, complex formation is favored, the H + CO_2 channel will dominate, favoring reaction 3f over reaction 3e, and minimizing generation of extra ^{13}CO. We have therefore used a ratio of 5:1 for the rate constants of reactions 3f and 3e.

Using these initial radical concentrations and rate constants, these reactions were numerically integrated separately for each 1-cm-deep volume along the cell axis and the results averaged. ^{13}CO from reaction 3b is produced on a few-hundred-μs time scale, but ^{13}CO from reactions 3d and 3e rises to concentrations comparable to the ^{13}CO produced from reaction 3b in about 0.1 s, indicating a problem that could invalidate our result. However, we have observed in our time-flight-experiments that the lifetime of O atoms can be strongly limited by reaction on untreated cell walls. Addition of a zeroth-order sink for O atoms

$$\mathrm{O} + \mathrm{wall} \rightarrow \mathrm{wall} \qquad (3\mathrm{i})$$

as an additional reaction with even a modest rate in the range 50−500 s^{-1} as shown in Figure 1 has a profound effect, dramatically reducing the production of ^{13}CO from reactions 3d and 3e. We have performed an experimental check on this calculation. Real-time measurements of CO concentrations using rovibrational absorptions on a faster-than-millisecond time scale are futile because of the slow equilibration rate among the internal degrees of freedom of CO. However, production of CO from reactions 3d−f occurs on much longer time scales (>100 ms), so that this time-dependence of the CO concentration is accessible using fast, sensitive lock-in amplifiers. Interference from buildup of ^{13}CO from dark reactions between laser pulses will appear as rising or falling ^{13}CO absorption after the sharp rise immediately following the UV laser pulse. Our ability to observe CO from one laser pulse removes any ambiguity caused by buildup of reaction products from multiple UV laser pulses. With an experimental arrangement as described above we were able to observe the time dependence for varying lengths of time of ^{13}CO absorption following irradiation of a fresh sample (with no ^{13}CO produced by any reactions) by one UV laser pulse with

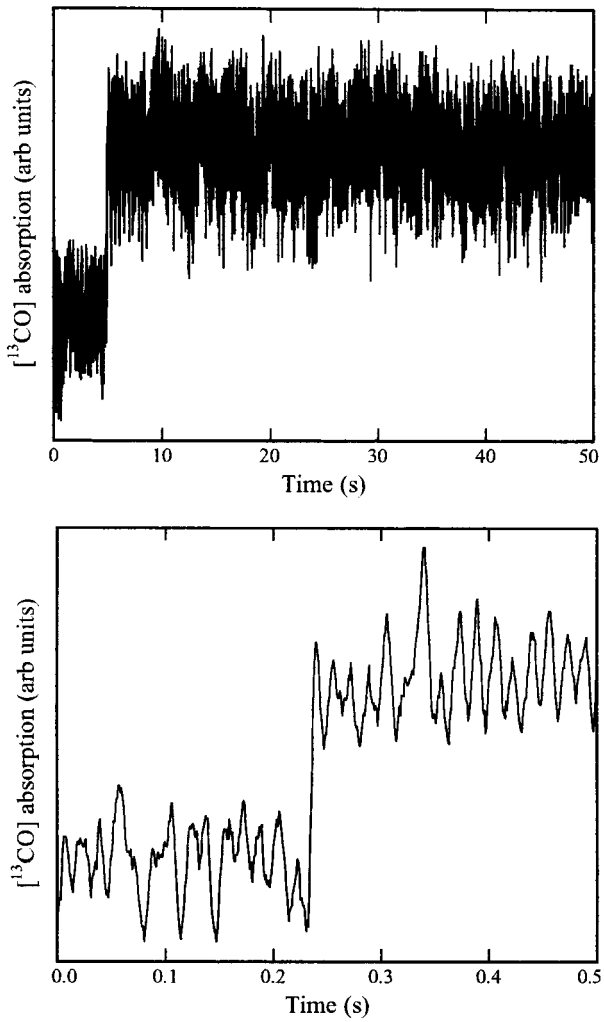

Figure 2. Time dependence of ^{13}CO absorption. Upper plot: profile of ^{13}CO absorption for 50 s following a *single* UV laser pulse; 4 mT (1.3×10^{14} molecules/cm^3) labeled acetone, 40 mT SO_2, 4.96 T Ar, 10 ms lock-in time constant. Lower plot: ^{13}CO absorption profile, average from five UV laser pulses, 3 ms time lock-in time constant.

a signal-to-noise ratio of about 5, adequate to demonstrate the result. Data are shown in Figure 2. After the fast production of ^{13}CO due to the reaction of methyl radicals with oxygen atoms, which cannot be temporally resolved with this setup, the CO concentration stays essentially flat over a time interval of up to 50 s (see Figure 2). Therefore, significant contributions to the ^{13}CO concentration from secondary reactions can be ruled out. The shape of the time-dependent ^{13}CO absorption following multiple UV laser pulses does not change, only the DC level of the absorption rises sharply as ^{13}CO concentration increases with each pulse. We therefore acquired averaged CO concentration profiles with improved signal-to-noise by averaging absorption from 5 to 10 pulses delivered at 2 Hz. The shape of the ^{13}CO concentration vs. time was the same as that observed from single pulses, but with improved signal-to-noise. Similar results were obtained by observing the shape of the CO concentration profile following a single 5-pulse group of UV pulses delivered at the maximum 20-Hz repetition rate for our laser. These experiments provide strong evidence that dark reactions between UV laser pulses do not materially affect the observed ^{13}CO yield.

If the reaction mixture is irradiated with a large number of excimer laser pulses and the concentrations of reaction products are permitted to build up, the influence from secondary photochemistry becomes evident. We followed the $^{13}C^{16}O$ and

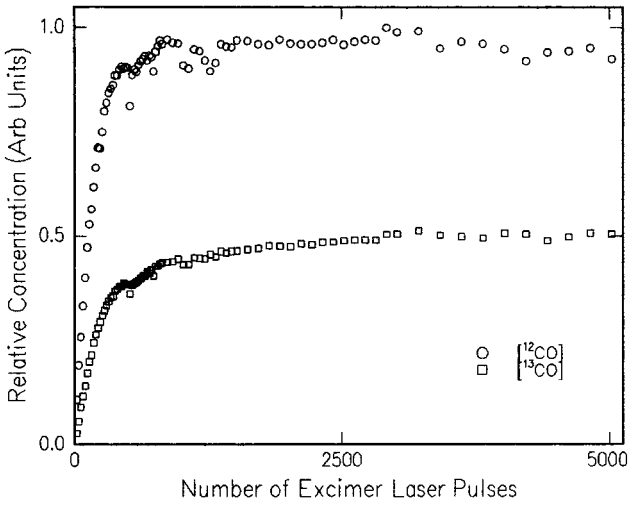

Figure 3. The relative concentrations of $^{12}C^{16}O$ (circles) and $^{13}C^{16}O$ (squares) as a function of the number of accumulated excimer laser pulses. The ratio of the concentrations of SO_2 to acetone in this experiment is 2.73. The reaction is followed for many more excimer laser pulses than for the data shown in Figures 4 and 5. See text. The amplitude of the slow rise of the $^{13}C^{16}O$ concentration contributes only ~10−15% to the total $^{13}C^{16}O$ concentration. Initial pressures: 1.36×10^{-2} Torr labeled acetone, 3.72×10^{-2} Torr SO_2, 4.90 T Ar.

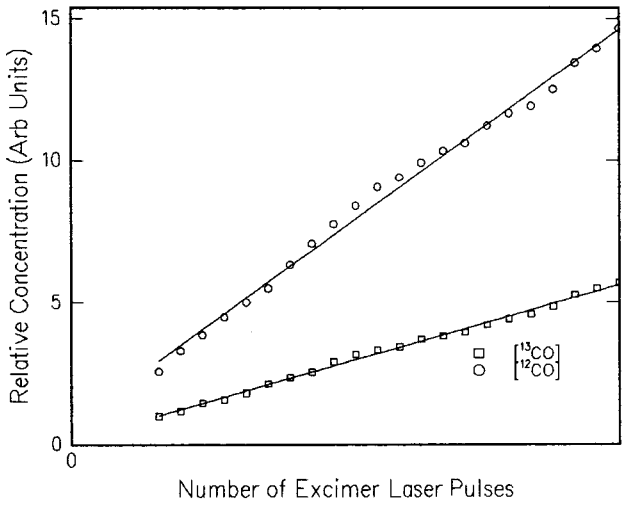

Figure 4. Concentrations of $^{12}C^{16}O$ (circles) and $^{13}C^{16}O$ (squares) as a function of the number of accumulated excimer laser pulses for a small number of excimer laser pulses. Conditions are cited in the text. The lines are linear least-squares fits to the data: [^{12}CO] slope = $2.78 \times 10^{-1} \pm 1.0 \times 10^{-2}$ (95%), intercept = $7.26 \times 10^{-1} \pm 3.2 \times 10^{-1}$ (95%), $r = +0.997$; [^{13}CO] slope = $1.10 \times 10^{-1} \pm 3.2 \times 10^{-3}$ (95%), intercept = $1.33 \times 10^{-1} \pm 1.0 \times 10^{-1}$ (95%), $r = +0.998$.

$^{12}C^{16}O$ concentrations for 5000 laser pulses (total pressure = 4.95 Torr, acetone pressure = 13.6 mTorr, SO_2 pressure = 37.2 mTorr). The concentrations of the two CO isotopologues rise linearly for the first 200−300 laser pulses. The concentration of $^{12}C^{16}O$ then levels off, while the concentration of $^{13}C^{16}O$ continues to rise another 10−15% of its total amplitude. See Figure 3. These data support a scheme where the concentration of $^{12}C^{16}O$ produced directly from acetone reaches a maximum when the acetone is completely consumed, but some more $^{13}C^{16}O$ is eventually produced from formaldehyde. The total concentration of $^{12}C^{16}O$ produced is consistent with the initial concentration of acetone, and the additional rise in $^{13}C^{16}O$ is sufficiently small not to exceed mass balance, but does not account for all of the ^{13}C available, even though in ref 1 the only substantial products detected were CO and formaldehyde.

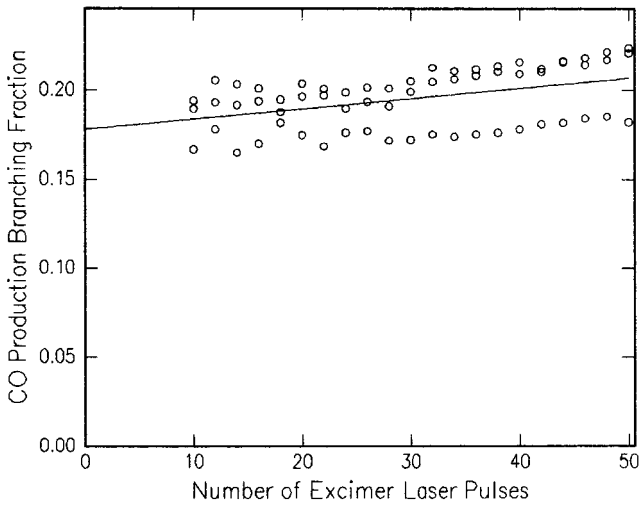

Figure 5. CO branching fraction for reactions 1 as a function of the number of accumulated excimer laser pulses. The line is a linear least-squares fit through the points: slope = $5.28 \times 10^{-4} \pm 6.1 \times 10^{-4}$ (95%), intercept = 0.18 ± 0.04 (95%), $r = +0.432$. Initial pressures: 4.12×10^{-3} Torr labeled acetone, $4.28\ 10^{-2}$ Torr SO_2, 4.91 Torr Ar.

Keeping the extent of reaction low (i.e., limiting the number of laser pulses), the concentrations of $^{13}C^{16}O$ and $^{12}C^{16}O$ rise essentially linearly with the number of excimer laser pulses, consistent with a mechanism where the main source of CO is the photolysis of acetone and reaction 1c. Such a plot of [$^{13}C^{16}O$] and [$^{12}C^{16}O$] vs. accumulated excimer laser pulses is shown in Figure 4. Initial concentrations in the reaction mixture were Ar, 4.94 T; acetone, 4.2×10^{-3} T; SO_2, 4.34×10^{-2} T. As will be described below, the determination of the product yield with this method depends only on concentration ratios but not on absolute concentrations. Thus experimental limitations such as zero-drift in the capacitance manometer used to make the premixed gas mixtures or to measure the pressure in the sample cell, and IR-detector drift during the experiment have no affect on the result.

Let the observed ratio of the area under the $^{12}C^{16}O$ line to that of the $^{13}C^{16}O$ line for natural abundance CO be M_{nat} (= $A^{nat}{}_{12}/A^{nat}{}_{13}$) and that for the reaction mixture be M_{rxn}. The real concentration ratio R in the reaction mixture is then $R = 89.66 \times M_{rxn}/M_{nat}$, where 89.66 is the ratio of ^{12}C to ^{13}C for natural abundance. Assuming no corrections are needed for reactions that scramble the products, the branching fraction, f_{CO} that describes CO from the $CH_3 + O$ reaction is just

$$f_{CO} = \frac{[^{13}C^{16}O]}{2[^{12}C^{16}O]} = \frac{1}{2R} \tag{4}$$

The factor of 2 in the denominator originates from the fact that the main channel of the photolysis of acetone at 193 nm leads to two methyl radicals and one CO molecule. According to Lightfoot et al.,[19] the overall yield for this process lies between 95% and 97% depending on the photon density. Other photolysis channels produce neither CO nor CH_3 directly and were therefore neglected in the analysis. Figure 5 is a plot of $1/2R$ for three combined experiments (all 4 mT labeled acetone, 40 mT SO_2, 5 T total pressure, balance Ar). Data representing fewer than five excimer laser pulses are omitted because the absolute values of these concentrations are comparable to the scatter in the measured values. The branching fraction, $1/2R$ extrapolated to zero excimer laser pulses is 0.18 ± 0.04, in excellent agreement with the TOFMS measurements. The branching fraction rises slightly with the accumulation of laser

pulses (and products). Even though we showed that the quantity of excess $^{13}C^{16}O$ from subsequent reactions of $^{13}CH_2O$ should be negligible under our conditions, our experiment is sensitive enough to detect a small rise in the branching fraction, which can be attributed to some secondary chemistry of ^{13}C-containing species. In any case, extrapolation of the branching fraction to zero laser pulses corrects for the rise.

The particular absorption lines used in this experiment probe $J = 17$ for $^{12}C^{16}O$, far from the room-temperature peak for the CO rotational distribution and $J = 6$ for $^{13}C^{16}O$, close to the room-temperature peak of the rotational distribution. This makes the comparison somewhat temperature sensitive (a one K error in measuring temperature introduces a 1% error in the measured ratio). The temperature of the laboratory during the experiment was held within the range 296 ± 1 K, so that the error introduced from this source was small.

The measurements in this work and the experiments discussed in ref 1 agree well, but neither provides much information about the mechanism of reactions (1) other than the relative importance of reaction 1c. There is a twofold benefit in this experiment compared to ref 1. First, the laser fluence employed here is about one-fifth that used in the earlier experiments, rendering secondary photolysis of the methyl radicals to produce methylene radicals even less likely (see also ref 13). Second, the higher bath gas pressure used here (5 Torr Ar compared to 1 Torr He) should reduce effects from the chemistry of vibrationally excited species, e.g., CH_3* from the photolysis of acetone or perhaps CH_2O* generated in reaction 1a. As discussed in ref 1 and in ref 4, the likely initial step in the reaction of CH_3 and O is the association of the reactants to form a highly excited methoxy radical. This radical has sufficient internal energy to eliminate molecular hydrogen, leading to HCO* that can decompose yielding CO, or to eliminate atomic hydrogen, producing CH_2O. Other possible mechanisms include isomerization of CH_3O* to CH_2OH*, followed by elimination of H and H_2. Since the features of the potential energy surfaces controlling these reactions are poorly known, there is as yet no definitive information available about the mechanism of CO formation.

Slagle et al.[3] found that reaction 1a was the only important reaction in the temperature range they studied, a range that included room temperature where our experiment was performed. Using a quadrupole mass spectrometer as their detector, they did not look for CO, so that a channel accounting for ~20% of reaction could easily be missed. On the other hand, Seakins and Leone[4] measured the overall CO yield to be 0.4 ± 0.2. The error limits for the two measurements just overlap. Finally, even though this experiment was performed using different experimental conditions than those in our TOFMS experiment, and the excellent agreement between the two experiments is remarkable.

Summary

We have measured the yield of CO from reactions (1) at room temperature. The result is a branching fraction of 0.18 ± 0.04, in excellent agreement with a previous measurement of the same quantity using time-of-flight mass spectrometry. We are extending these measurements to higher temperatures using both TOFMS and IR diode-laser absorption. We expect that the TOFMS measurements will be more accurate at higher temperatures than measurements using IR absorption because the absorption measurements will eventually be limited by line width considerations, thermolysis in a static cell, and the sensitivity to temperature of concentration measurements using rovibrational transitions probing states far from the peak of the equilibrium rotational distribution combined with our ability to generate a flat well-defined temperature profile in the sample cell.

Acknowledgment. This work was performed at Brookhaven National Laboratory under Contract DE-AC02-98CH10886 with the U.S. Department of Energy and supported by its Division of Chemical Sciences, Office of Basic Energy Sciences. Support for G.W.F. was provided by the U.S. Department of Energy under grant DE-FG02-88ER13937. We gratefully acknowledge the contribution of a reviewer whose suggestions led to greatly strengthening our arguments regarding potential CO production from secondary reactions.

References and Notes

(1) Fockenberg, C.; Hall, G. E.; Preses, J. M.; Sears, T. J.; Muckerman, J. T.; *J. Phys. Chem. A* **1999**, *103*, 5722.

(2) Fockenberg, C.; Bernstein, H. J.; Hall, G. E.; Muckerman, J. T.; Preses, J. M.; Sears, T. J.; Weston, R. E., Jr. *Rev. Sci. Instrum*. **1999**, *70*, 3259.

(3) Slagle, I. R.; Sarzyński, D.; Gutman, D. *J. Phys. Chem.* **1987**, *91*, 4375.

(4) Seakins, P. W.; Leone, S. R. *J. Phys. Chem*. **1992**, *96*, 4478.

(5) Smith, G. P.; Golden, D. M.; Frenklach, M.; Moriarty, N. W.; Eiteneer, B.; Goldenberg, M.; C.; Bowman, C. T.; Hanson, R. K.; Song, S.; Gardiner, W. C., Jr.; Lissianski, V. V.; Qin, Z. http://www.me.berkeley.edu/gri_mech/.

(6) Kee, R. J.; Rupley, F. M.; Miller, J. A. *Sandia Report SAND89-8009B · UC-70*6, Chemkin-II: A Fortran Chemical Kinetics Package for the Analysis of Gas-Phase Chemical Reactions, Sandia National Laboratories, **1989**.

(7) Rudolph, R. N.; Hall, G. E.; Sears, T. J. *J. Chem. Phys.* **1996**, *105*, 7889.

(8) Guelachvili, G.; Rao, K. N. *Handbook of Infrared Standards*; Academic Press: Orlando, **1979**; pp 510−11.

(9) Lide, D. R., ed. *Handbook of Chemistry and Physics 75th ed.*; CRC Press: Boca Raton, **1994**; p 1−10.

(10) Baulch, D. L.; Cobos, J.; Cox, R. A.; Frank, P.; Hayman, G.; Just, Th.; Kerr, J. A.; Murrels, T.; Pilling, M. J.; Troe, J.; Walker, R. W.; Warnatz, J. *J. Phys. Chem.* Ref. Data **1994**, *23*, 980.

(11) Manatt, S. L.; Lane, A. *J. Quant. Spectrosc. Radiat. Transfer* **1993**, *50*, 267.

(12) Phillips, L. F. *J. Phys. Chem.* **1981**, *85*, 3994.

(13) Min, Z.; Quandt, R. W.; Wong, T-. H.; Bersohn, R. *J. Chem. Phys.* **1999**, *111*, 7369.

(14) Baulch, D. L.; Cobos, C. J.; Cox, R. A.; Esser, C.; Frank, P.; Just, Th.; Kerr, J. A.; Pilling, M. J.; Troe, J.; Walker, R. W.; Warnatz, J. *J. Phys. Chem. Ref. Data* **1992**, *21*, 411.

(15) Le Calve, S.; Hitier, D.; Le Bras, G.; Mellouki, A. *J. Phys. Chem. A* **1998**, *102*, 4579.

(16) Singleton, D. L.; Cvetanovic, R. J. *J. Phys. Chem. Ref. Data* **1988**, *17*, 1377.

(17) Bradley, K. S.; Schatz, G. C. *J. Chem. Phys*. **1997**, *106*, 464.

(18) Schatz, G. C., private communication.

(19) Lightfoot, P. D.; Kirwan, S. P.; Pilling, M. J. *J. Phys. Chem*. **1988**, *92*, 4938.